

Published in final edited form as:

Hepatology. 2014 June ; 59(6): 2263–2275. doi:10.1002/hep.26993.

## Cholangiocyte Senescence by Way of N-Ras Activation Is a Characteristic of Primary Sclerosing Cholangitis

James H. Tabibian<sup>\*</sup>, Steven P. O'Hara<sup>\*</sup>, Patrick L. Splinter, Christy E. Trussoni, and Nicholas F. LaRusso

Division of Gastroenterology and Hepatology, and the Mayo Clinic Center for Cell Signaling in Gastroenterology, Mayo Clinic, Rochester, MN

### Abstract

Primary sclerosing cholangitis (PSC) is an incurable cholangiopathy of unknown etiopathogenesis. Here we tested the hypothesis that cholangiocyte senescence is a pathophysiologically important phenotype in PSC. We assessed markers of cellular senescence and senescence-associated secretory phenotype (SASP) in livers of patients with PSC, primary biliary cirrhosis, hepatitis C, and in normals by fluorescent in situ hybridization (FISH) and immunofluorescence microscopy (IFM). We tested whether endogenous and exogenous biliary constituents affect senescence and SASP in cultured human cholangiocytes. We determined in coculture whether senescent cholangiocytes induce senescence in bystander cholangiocytes. Finally, we explored signaling mechanisms involved in cholangiocyte senescence and SASP. *In vivo*, PSC cholangiocytes expressed significantly more senescence-associated p16<sup>INK4a</sup> and  $\gamma$ H2A.x compared to the other three conditions; expression of profibrogenic SASP components (i.e., IL-6, IL-8, CCL2, PAI-1) was also highest in PSC cholangiocytes. *In vitro*, several biologically relevant endogenous (e.g., cholestane 3,5,6 oxysterol) and exogenous (e.g., lipopolysaccharide) molecules normally present in bile induced cholangiocyte senescence and SASP. Furthermore, experimentally induced senescent human cholangiocytes caused senescence in bystander cholangiocytes. N-Ras, a known inducer of senescence, was increased in PSC cholangiocytes and in experimentally induced senescent cultured cholangiocytes; inhibition of Ras abrogated experimentally induced senescence and SASP.

**Conclusion**—Cholangiocyte senescence induced by biliary constituents by way of N-Ras activation is an important pathogenic mechanism in PSC. Pharmacologic inhibition of N-Ras with a resultant reduction in cholangiocyte senescence and SASP is a new therapeutic approach for PSC.

---

Primary sclerosing cholangitis (PSC) is an idiopathic, chronic cholangiopathy characterized by biliary fibroinflammation,<sup>1,2</sup> median liver transplantation (LT)-free survival of 12 years,<sup>3</sup>

---

Copyright © 2014 by the American Association for the Study of Liver Diseases.

Address reprint requests to: N.F. LaRusso, Division of Gastroenterology and Hepatology, Mayo Clinic College of Medicine, 200 First Street, SW, Rochester, MN 55905. larusso.nicholas@mayo.edu.

<sup>\*</sup>These authors contributed equally to this work.

Potential conflict of interest: Nothing to report.

### Supporting Information

Additional Supporting Information may be found in the online version of this article at the publisher's website.

and a predisposition to cholangiocarcinoma (CCA).<sup>4</sup> While PSC has no established pharmacotherapy, LT can be an effective treatment for this disease, although PSC and/or CCA may recur post-LT.<sup>4,5</sup> Therefore, given the morbidity and mortality of PSC, the lack of effective pharmacotherapy, and the issue of post-LT disease recurrence, a better understanding of its pathogenesis and identification of new therapeutic molecular targets are needed.

PSC is considered a complex, idiopathic disorder with multiple potential pathogenic components, including enteric microbially derived molecules such as lipopolysaccharide (LPS).<sup>1</sup> Enterically derived LPS reaches the liver through the portal circulation, is excreted into bile in a bioactive form, and accumulates in cholangiocytes in PSC liver tissue.<sup>6,7</sup> We previously reported that cultured normal human cholangiocytes (NHCs) can be activated by LPS through Toll-like receptor (TLR)-dependent pathways,<sup>8</sup> culminating in secretion of proinflammatory cytokines (e.g., interleukin [IL]-6), as can be seen in PSC.<sup>9–11</sup> Indeed, PSC cholangiocytes demonstrate persistence of this proinflammatory phenotype *ex vivo*.<sup>12</sup> While these cholangiocyte proinflammatory responses are believed important in the pathogenesis of PSC, their underlying mechanisms and consequences remain poorly understood.

Recently, the phenomenon of cellular senescence has been shown to be an important pathologic process in a number of conditions of diverse etiologies, including atherosclerosis, osteoarthritis, and chronic obstructive pulmonary disease.<sup>13,14</sup> Senescent cells are irreversibly arrested in G<sub>1</sub> phase of the cell cycle and thus no longer replicate.<sup>15</sup> Senescence can be triggered by a number of stimuli, including strong mitogenic or oncogenic signals, telomere shortening, and/or nontelomeric DNA damage from exogenous or endogenous molecules; such molecules can then activate pathways, notably p16<sup>INK4a</sup>, that silence cell cycle-associated loci and initiate a cellular senescence response.<sup>14,16</sup> Although this generally serves as a mechanism to inhibit propagation or neoplastic transformation of damaged cells, senescent cells can also transition to a potentially pathologic state of proinflammatory cytokine (e.g., IL-6) and chemokine (e.g., IL-8) hypersecretion, referred to as a senescence-associated secretory phenotype (SASP).<sup>17</sup> By way of these secreted molecules, SASP cells can alter their microenvironment, reinforce the senescent phenotype, and initiate injurious cellular responses.<sup>13,14,18–20</sup>

In our previous work using human cholangiocytes, we demonstrated that ligand-induced activation of plasma membrane-localized TLRs not only activates nuclear factor kappa B (NF- $\kappa$ B) through canonical pathways, but also rapidly activates N-Ras (but not other Ras isoforms) in a TRAF6-independent manner.<sup>8</sup> Notably, persistent Ras activation is a well-characterized inducer of cellular senescence.<sup>17,21</sup> Moreover, activated (or “reactive”) cholangiocytes exhibit proinflammatory features<sup>8,11,22</sup> similar to SASP cells; whether this represents stress-induced cholangiocyte senescence and SASP, and how these cellular processes may contribute to cholangiocyte pathobiology, has been underexplored in the pathogenesis of PSC.<sup>2</sup>

Therefore, in work described herein, we: 1) investigated whether cholangiocytes in PSC liver exhibit evidence of cellular senescence and SASP; 2) developed a novel, *in vitro* model of persistent insult-induced NHC senescence to interrogate the induction of cholangiocyte

senescence and progression to SASP; 3) explored the possibility of senescent cholangiocytes inducing senescence of bystander cholangiocytes; and 4) identified a significant role for N-Ras signaling in cholangiocyte senescence and potentially the pathogenesis of PSC. Our cumulative data suggest that non-replicative cholangiocyte senescence induced by biliary constituents by way of N-Ras activation is an important pathophysiologic feature of PSC and that pharmacologic abrogation of these pathways and the cholangiocyte SASP may represent a novel, potential therapeutic strategy for PSC.

## Materials and Methods

This study was approved by the Mayo Clinic Institutional Review Board and Institutional Animal Care and Use Committee.

### Liver Tissues

Twenty-eight liver tissue specimens consisting of nine PSC, six primary biliary cirrhosis (PBC), six hepatitis C (HCV), and seven normals from surgical resection or explant were used. Median patient ages in these four groups were 46, 46, 41, and 47 years, respectively. Diseased specimens fulfilled clinical, serological, histological, and/or cholangiographic criteria for their respective diagnoses and had stage IV (i.e., cirrhotic stage) fibrosis. All PSC patients were negative for biochemical, imaging, or histologic evidence of cholangiocarcinoma, while five of nine had inflammatory bowel disease. Liver specimens were fixed in 10% neutral buffered formalin, embedded in paraffin, and sectioned (4  $\mu$ m) for the following experiments as well as for laser capture microdissection (LCM) using a Veritas microdissection instrument (Arcturus, Mountain View, CA) as described previously.<sup>23,24</sup>

### Confocal Immunofluorescence (IF) Microscopy

Confocal IF microscopy was performed with a Zeiss LSM 510 confocal microscope with a 63 $\times$  oil objective as previously described (see Supporting Methods).<sup>25</sup> Briefly, unstained liver sections were deparaffinized and rehydrated, boiled in antigen unmasking solution (Vector Laboratories, Burlingame, CA), quenched with Image-iT FX signal enhancer (Invitrogen, Grand Island, NY), and blocked for 1 hour at room temperature. Slides were then incubated overnight at 4 $^{\circ}$ C with various antibodies (see Supporting Methods). Adobe Photoshop CS3 (Adobe Systems, San Jose, CA) was used to quantitate fluorescence intensity within cholangiocytes. For  $\gamma$ H2A.x quantitation, the percentage of cholangiocytes per duct with  $>4$   $\gamma$ H2A.x-positive nuclear foci was calculated.<sup>27</sup>

### Fluorescence In Situ Hybridization (FISH)

Telomere FISH was performed using PNA TelC-FITC (PNA Bio, Thousand Oaks, CA) with tyramide signal amplification based on the manufacturer's protocol and previously described methods (see Supporting Methods).<sup>28,29</sup> Briefly, liver sections were deparaffinized, rehydrated, boiled in citrate buffer, prehybridized, heat-denatured, and hybridized to TelC telomere probe diluted in hybridization solution. Antifluorescein peroxidase-conjugated antibody (Rockland Immunochemicals, Gilbertsville, PA) was added to the slides. Slides were washed, incubated in tyramide amplification solution (PerkinElmer, Waltham, MA),

and washed again. Fluorescent signals were quantitated for each cholangiocyte nucleus and divided by the DAPI signal for the corresponding nucleus.<sup>28,30</sup>

Detection of p16<sup>INK4a</sup> messenger RNA (mRNA) was performed as described previously (see Supporting Methods).<sup>31</sup> Briefly, liver sections were deparaffinized, rehydrated, boiled in buffer, prehybridized, and incubated with either a scrambled probe or p16<sup>INK4a</sup> LNA probe (Exiqon, Woburn, MA). Fluorescence intensity was visualized and quantitated as described above.

### Cell Culture and *In Vitro* Model of Senescence

NHCs (extensively characterized, low-passage human biliary epithelia cells isolated from normal liver<sup>32</sup>) were a gift from Dr. Medina (University of Navarra, Pamplona, Spain). Microbially derived agonists (i.e., exogenous insults) were individually added to NHC media at the following concentrations: LPS (1–200 ng/mL), FSL1 (1 µg/mL), flagellin (10 µg/mL), heat-killed *Listeria monocytogenes* (HKLM; 10<sup>8</sup> cells/mL), and Pam3CSK4 (1 µg/mL) (Invivogen, San Diego, CA).<sup>8</sup> Nonmicrobially derived agonists (i.e., endogenous insults) were added at the following concentrations: H<sub>2</sub>O<sub>2</sub> (50 nM), cholestane-3β, 5α, 6α-triol (5–25 µM), 22-hydroxycholesterol (20 µM), deoxycholic acid (25 µM), lithocholic acid (10 µM), and adenosine triphosphate (5 µM) (Sigma-Aldrich, St. Louis, MO). Media and appropriate agonists were replaced every 24–48 hours for up to 10 days. Controls were grown either in complete media or media containing vehicle (dimethyl sulfoxide [DMSO]).

For Ras and NF-κB inhibitor studies, farnesylthiosalicylic acid (FTS; Cayman Chemicals, Ann Arbor, MI) and SN50 (Millipore, Billerica, MA) were used at a final concentration of 5 µM and 20 µM, respectively. For transfections, NHCs were transfected with the p16<sup>INK4a</sup> promoter-driven red fluorescent protein, enhanced green fluorescent protein (pEGFP-N1), or pCGN (N-Ras 12D) constitutively active plasmids using FuGENE HD (Roche Diagnostics, Indianapolis, IN) following the manufacturer's protocol. All culture-based experiments were performed at least in triplicate.

For the coculture senescence model, NHCs were plated and agonists (H<sub>2</sub>O<sub>2</sub> or LPS) were added to media as above (“directly treated senescent cholangiocytes”). In a separate 6-well plate, bystander cholangiocytes were plated onto coculture filter inserts. At day 7, the directly treated senescent cholangiocytes were washed 5 times in phosphate-buffered saline (PBS), and complete media was added. The coculture filter inserts were transferred to the 6-well plate with the directly treated senescent cholangiocytes and incubated for an additional 7 days. Senescence-associated β-galactosidase (SA-β-gal) staining was performed as described below on both the directly treated senescent cholangiocytes and the bystander cholangiocytes.

### Cytochemical Staining for SA-β-Gal

NHCs grown in 6-well plates were fixed, rinsed, and stained using the SA-β-gal cellular senescence assay kit (Cell Biolabs, San Diego, CA) following the manufacturer's protocol and as previously described.<sup>33</sup> The percentage of SA-β-gal-positive NHCs was determined

for each condition using a 20 × objective and bright field illumination of five randomly selected areas.

### **RNA Extraction and Quantitative Reverse-Transcription Polymerase Chain Reaction (RT-PCR)**

Total RNA was extracted from NHCs with Trizol (Invitrogen) and 2.5 µg of total RNA was reverse-transcribed into complementary DNA (cDNA) using SuperScript III First-Strand Synthesis System for RT-PCR (Invitrogen) following the manufacturer's protocol. Quantitative (q)RT-PCR was performed using the Light Cycler Fast Start DNA Master<sup>Plus</sup> SYBR Green I kit (Roche) as previously described.<sup>8</sup> Primer sequences used are provided in Supporting Table 1. Samples were normalized to 18s rRNA.

### **Assessment of Lysosomal Content**

Lysosomal content was quantitated using LysoTracker stain (Invitrogen) following the manufacturer's protocol. Briefly, LysoTracker was added to media at a final concentration of 75 nM, incubated for 60 minutes at 37°C, and visualized by fluorescence microscopy. Fluorescence intensity was quantitated as above.

### **Enzyme-Linked Immunosorbent Assay (ELISA)**

Culture medium was centrifuged to remove cellular debris, and 100 µL of cleared medium from NHCs in the presence or absence of LPS was used in the Mix-N-Match ELISA following the manufacturer's instructions (SABiosciences) and as previously described.<sup>8</sup> ELISAs were read using a 450-nm wavelength against a 630-nm reference wavelength. Experimental samples were normalized to the respective controls.

### **Western Blotting for p16<sup>INK4a</sup> and Activated N-Ras**

Total protein was isolated from NHCs using M-PER reagent containing protease inhibitors (Roche). Immunoblots were performed using primary antibodies to p16<sup>INK4a</sup> or N-Ras (Santa Cruz Biotechnology, Santa Cruz, CA) as previously described.<sup>8</sup> N-Ras activation was assessed in NHCs cultured in the presence or absence of LPS for 0, 1, 2, 6, and 10 days using a Ras activation kit (Cytoskeleton, Denver, CO) following the manufacturer's protocol and as previously described (see Supporting Methods).<sup>8</sup>

### **Statistical Analysis**

All data are reported as the mean (or fold change in mean) ± standard error. Statistical analyses were performed with Student *t* test or the Mann-Whitney *U* test using JMP statistical software (SAS Institute, Cary, NC). Tests were two-tailed and *P* < 0.05 was considered statistically significant. Bonferroni adjustment was made to *P*-values for multiple comparisons.

## Results

### Cholangiocytes in PSC Liver Exhibit Features of Cellular Senescence

We first determined whether histologic features consistent with cholangiocyte senescence are present in normal, HCV, PBC, and PSC liver. Using FISH and confocal IF microscopy, we assessed: p16<sup>INK4a</sup> mRNA, histone  $\gamma$ H2A.x foci, and Ki-67 protein. p16<sup>INK4a</sup> mRNA expression was significantly greater in PSC cholangiocytes compared to PBC (3.1-fold,  $P < 0.01$ ), HCV, and normal (both  $>20$ -fold,  $P < 0.01$ ) (Fig. 1A,B). Thus, cholangiocytes in PSC exhibit increased p16<sup>INK4a</sup> expression, consistent with senescence.

We next investigated the presence of  $\gamma$ H2A.x nuclear foci, which accumulate at DNA double-strand breaks and are a biomarker of cellular senescence.<sup>34</sup> PSC liver had the greatest proportion (47.3%) of  $\gamma$ H2A.x foci-positive cholangiocytes (Fig. 1C,D), representing a 1.5, 3.2, and 5.9-fold increase over PBC ( $P < 0.05$ ), HCV ( $P < 0.01$ ), and normal ( $P < 0.01$ ), respectively. Moreover,  $\gamma$ H2A.x-positive cholangiocytes in PSC liver were negative for cell proliferation marker Ki-67, as expected of senescent cells (Supporting Fig. 1A,B).<sup>34</sup> These findings suggest a pathogenic role for DNA damage-induced cholangiocyte senescence in PSC.

To further explore the senescent phenotype, we assessed whether senescence in PSC cholangiocytes was replicative or nonreplicative. Replicative senescence is induced by a loss of telomere repeat sequences; nonreplicative senescence is telomere shortening-independent and is considered stress-induced. Using FISH, we found that telomere length is maintained in PSC cholangiocytes but reduced in PBC cholangiocytes (Fig. 2A,B); these data in PBC are consistent with a prior report.<sup>30</sup> The relatively preserved telomere length of cholangiocytes in PSC liver and the similar ages between groups suggest that, unlike in PBC, PSC cholangiocyte senescence may be stress-induced rather than initiated by telomere shortening.

### PSC Cholangiocyte Protein Expression Is Consistent With SASP

Senescent cells may progress to the SASP, a persistent hypersecretory state characterized by increased expression of profibroinflammatory molecules. Using confocal IF microscopy, we investigated four known SASP components; all four were highly expressed in PSC cholangiocytes (Fig. 3A,B). Specifically, IL-6 expression was significantly higher in PSC cholangiocytes compared to PBC, HCV, and normal (9.1, 5.6, and  $>20$ -fold, respectively, all  $P < 0.01$ ). Similarly, IL-8 expression was significantly higher in PSC cholangiocytes compared to PBC, HCV, and normal (3.0, 2.5, and 7.9-fold, respectively, all  $P < 0.01$ ). CCL2 expression was significantly higher in PSC cholangiocytes compared to normal and HCV (both  $>10$ -fold,  $P < 0.05$ ) but not compared to PBC. Finally, PAI-1 expression was significantly higher in PSC cholangiocytes compared to PBC, HCV, and normal (3.0, 4.4, and 8.7-fold, respectively, all  $P < 0.01$ ). In addition to confocal IF microscopy, we assessed SASP marker mRNA in cholangiocytes isolated from liver section using LCM (Supporting Fig. 2A–C). We found that, on average, IL-6 and IL-8 expression were 5.2- and 8.4-fold higher in PSC cholangiocytes compared to normal ( $P < 0.05$  and  $P < 0.01$ , respectively). Collectively, these findings: 1) demonstrate that known SASP proteins are expressed by

PSC cholangiocytes and increased compared to other conditions; and 2) support the concept that cholangiocytes may directly contribute to the biliary fibroinflammation observed in PSC.<sup>2</sup>

### ***In Vitro* Model of Stress-Induced Cholangiocyte Senescence**

We developed an *in vitro* model to test the ability of persistent (10 day) treatment with biologically relevant stressors to induce NHC senescence (Supporting Fig. 3A). Two previously reported models of cultured cholangiocyte senescence used murine cholangiocytes, tested fewer stressors, and were assessed at only 4–8 days.<sup>35,36</sup> In our model, the exogenous stressors LPS (200 ng/mL), Flagellin, FSL-1, HKLM, and Pam3CSK4 significantly induced NHC senescence as determined by SA- $\beta$ -gal expression, a widely used marker of senescent cells (Fig. 4A,B). The endogenous stressors H<sub>2</sub>O<sub>2</sub> and oxysterol cholestane-3 $\beta$ , 5 $\alpha$ , 6 $\alpha$ -triol also induced significant NHC senescence; 22-hydroxycholesterol, deoxycholic and lithocholic acid, and adenosine triphosphate did not. Given our previous experience with LPS as well as the evidence supporting its role in PSC and other inflammatory cholangiopathies,<sup>2,6,37,38</sup> our subsequent studies employed LPS as the experimental stressor. Notably, even with low doses of LPS, cholangiocytes transition to a senescent state, albeit at a slower rate as compared to higher doses (Supporting Fig. 3B).

### **Persistent Treatment With LPS Induces Expression of Multiple Senescence Markers in Cholangiocytes *In Vitro***

To better characterize the time course of LPS-induced NHC senescence induction in our *in vitro* model, we evaluated several senescence markers at 1, 6, and 10 days of treatment compared to control. Persistent LPS treatment induced p16<sup>INK4a</sup> mRNA expression in NHCs at days 6 and 10 (both >5 fold,  $P < 0.05$ ) (Fig. 4C). Similarly, persistent LPS treatment induced expression of p21 (cyclin-dependent kinase inhibitor 1), another marker and mediator of cellular senescence (data not shown). We also observed an initial increase in Ki-67 mRNA expression at day 1 (2.5-fold,  $P < 0.05$ ), consistent with acute LPS treatment-induced reactivity,<sup>8,39</sup> followed by a progressive decrease (0.8-fold difference at day 10,  $P > 0.05$ ), consistent with a nonreplicative state (Supporting Fig. 3C). The percentage of SA- $\beta$ -gal-positive cholangiocytes increased significantly at days 6 (3.6-fold,  $P < 0.05$ ) and 10 (5.9-fold,  $P < 0.05$ ) in LPS-treated NHCs (Fig. 5A,B). Additionally, we assessed NHC lysosomal content, a biomarker of cellular senescence,<sup>40</sup> and observed a significant increase in lysosomal content at days 6 and 10 (1.5 and 1.7-fold, respectively, both  $P < 0.05$ ) (Fig. 5C,D). Together, these findings indicate LPS-induced NHC senescence induction during the course of our *in vitro* model.

To further follow the induction of senescence in our model, we cotransfected NHCs with p16<sup>INK4a</sup> promoter-driven RFP reporter construct and EGFP, the latter as transfection control. We found a significant increase in the ratio of RFP- to EGFP-positive cells at days 6 and 10 (both >5-fold,  $P < 0.05$ ) (Fig. 5E,F), thus corroborating our above findings.

## LPS Treatment-Induced Cholangiocyte Senescence Leads to Expression of SASP Components

We next assessed whether NHCs in our *in vitro* model progress to the SASP. We first evaluated mRNA expression of three SASP components, IL-6, IL-8, and CCL2; all were significantly increased at day 10 in LPS-treated NHCs compared to control (all  $P < 0.05$ ) (Fig. 6A–C). Next, using ELISA, we measured protein expression of the same three SASP components in culture media at day 10. Similar to mRNA, all three SASP proteins were significantly more expressed in LPS-treated compared to control media (all  $P < 0.05$ ) (Fig. 6D). Collectively, these data indicate that experimentally induced senescent NHCs can progress to SASP *in vitro*.

## Senescent Cholangiocytes Induce Senescence of Bystander Cholangiocytes *In Vitro*

In some cell culture models, senescent cells can induce senescence of bystander cells.<sup>41,42</sup> We therefore developed a cholangiocyte coculture model to assess whether senescent cholangiocytes can induce senescence of bystander cholangiocytes (Supporting Fig. 4A). We found that bystander cholangiocytes demonstrate significantly increased expression of SA- $\beta$ -gal when exposed to cholangiocytes directly treated with H<sub>2</sub>O<sub>2</sub> or LPS (Supporting Fig. 4B,C), thus representing a mechanism for chronic, progressive hepatobiliary injury in PSC.

## Cholangiocyte Senescence Is N-Ras-Dependent and Is Abrogated by Ras Inhibitors

We previously showed that short-term treatment of cultured NHCs with LPS results in activation of the well-described inducer of senescence, Ras, specifically, the N-Ras isoform.<sup>8</sup> We thus assessed whether N-Ras is also activated in cholangiocytes in PSC liver. Using confocal IF microscopy, we found that: 1) N-Ras and activated Ras are both expressed significantly more in cholangiocytes in PSC compared to control liver (1.8- and 3.9-fold, respectively, both  $P < 0.05$ ) (Fig. 7A,B); and that 2) N-Ras colocalizes with activated Ras (Fig. 7A). N-Ras and activated Ras were not significantly increased in cholangiocytes in PBC or HCV liver (data not shown). These findings suggest increased expression and activation of N-Ras in PSC cholangiocytes and a potential role for activated N-Ras signaling in the pathogenesis of PSC.

We next investigated whether N-Ras activation occurs in our *in vitro* model of NHC senescence. N-Ras expression and activation peaked at day 6 of LPS treatment and remained elevated through day 10 (Fig. 7C,D). Based on these results and the role of Ras in senescence in other cell types, we hypothesized that N-Ras activation may induce NHC senescence. Indeed, we found that transfected NHCs expressing constitutively active N-Ras showed a significantly increased proportion of SA- $\beta$ -gal-positive cells at day 10 compared to control (Fig. 7E). To further examine this relationship, we assessed the effect of pharmacologic inhibition of Ras on the induction of NHC senescence. We found that administration of the Ras inhibitor, FTS, reduced the proportion of SA- $\beta$ -gal-positive NHCs at day 10 of LPS treatment (Fig. 7E). We also assessed the effect of NF- $\kappa$ B inhibition given its role as an effector of TLR activation and reported importance in senescence in other cell types. However, we did not observe a significant reduction in the proportion of SA- $\beta$ -gal-positive NHCs (Fig. 7E). Collectively, these data suggest that: 1) LPS-induces N-Ras



activation-mediated NHC senescence *in vitro*; and 2) LPS-induced NHC senescence can be abrogated by Ras inhibition.

## Discussion

The major findings of this study are: 1) *in vivo*, PSC cholangiocytes exhibit features consistent with nonreplicative (i.e., stress-induced) senescence and the SASP; 2) *in vitro*, persistent exposure to LPS and other exogenous and endogenous insults can induce senescence and progression to the SASP in human cholangiocytes; 3) senescent human cholangiocytes are capable of inducing senescence of bystander cholangiocytes in a coculture system; 4) N-Ras activation is increased in PSC cholangiocytes and contributes to senescence of NHCs *in vitro*; and 5) pharmacologic inhibition of Ras but not NF- $\kappa$ B can abrogate induction of senescence in cultured human cholangiocytes. These data have implications not only for the pathogenesis of PSC, but also for *in vitro* and *in vivo* interrogation of the pathways involved in the induction of cholangiocyte senescence and the identification of novel therapeutic targets.

Cellular senescence was originally described as a process that limits proliferation of human cells in culture.<sup>43</sup> It is now widely accepted as a mechanism to irreversibly block expansion of aged (i.e., shortened telomere) or damaged (e.g., DNA double-strand breaks) cells. Under these conditions, detection of genomic damage initiates the DNA damage response (DDR), which identifies DNA lesions, signals their presence, and promotes genomic repair.<sup>44</sup> If the damage is repaired, the DDR subsides, allowing normal cellular function to resume; if the damage is not repaired, the cell undergoes apoptosis or enters a senescent state, thus inhibiting neoplastic transformation.<sup>15</sup> Senescence and the SASP also contribute to tissue repair processes<sup>45</sup>; however, persistence of senescent and SASP cells can have pathologic consequences,<sup>13,14</sup> and current paradigms suggest that senescent and SASP cells may directly contribute to tissue damage and disease through cellular dysfunction (of the senescent and neighboring cells), structural (e.g., matrix) derangement, a reduced pool of regeneration-competent cells, and abnormal leukocyte chemotaxis.<sup>13</sup> The growing recognition of the potential importance of cellular senescence and the SASP in tissue inflammation, injury, and the pathogenesis of diseases of diverse etiologies, as well as our finding that ligand-induced activation of plasma membrane TLRs activates the well-known inducer of senescence, N-Ras, was the underlying rationale for our hypothesis that this phenomenon might be pathophysiologically important in PSC.

In our study, we examined several senescence markers and SASP components to assess their presence in and relevance to PSC. We found markers of cholangiocyte senescence to be more abundant in PSC cholangiocytes compared to other conditions. We also discovered that, unlike in PBC, cholangiocyte senescence in PSC appears to occur independent of telomere shortening; this suggested to us the possibility of an alternative mechanism, i.e., insult-induced (nonreplicative) senescence. While the precise mechanism by which PSC cholangiocytes up-regulate p16 and enter a senescent state remains unresolved, our data support a role for Ras activation, a known mediator of telomere-independent senescence, which may be induced by endogenous or exogenous biliary constituents, as we have shown. With respect to cholangiocyte SASP, we found that, as with senescence markers, profibroin-

flammatory SASP components were most abundantly expressed in PSC cholangiocytes. To our knowledge, this represents the first characterization of multiple SASP components in PSC; a prior study in PBC examined and showed increased expression of these components (CCL2).<sup>19</sup> We also developed an *in vitro* model of persistent insult-induced cholangiocyte senescence using NHCs and characterized the induction of senescence and SASP over 10 days. By adapting this model into a coculture assay, we showed with direct experimental evidence that senescent human cholangiocytes are able to induce senescence of bystander cholangiocytes. Collectively, our data suggest a possible role for nonreplicative senescence and SASP in the pathogenesis of PSC, while also providing novel information on both the mechanism and cellular consequences of these phenomena.

Although the causes and consequences of cholangiocyte senescence remain incompletely understood, accumulating evidence suggests that senescent cells, albeit proliferatively arrested, remain metabolically active and play an important role in microenvironment modulation through increased expression of cytokines, chemokines, and profibrotic factors.<sup>17-20,41</sup> Applying this knowledge and our experimental findings to PSC, various signaling molecules may directly participate in chronic biliary injury and fibrosis by way of eliciting cholangiocyte reactivity and ductular reaction, which in some circumstances may ultimately result in induction of cholangiocyte senescence. Furthermore, because senescent cholangiocytes do not proliferate in response to injury, and because they persist *in situ* (i.e., not efficiently cleared by immune mechanisms or apoptosis), their accumulation and signaling may disrupt the balance between cholangiocyte injury and regeneration and drive progressive bile duct injury and ductopenia, both of which are characteristic of PSC.<sup>2</sup> Furthermore, as evidenced by our coculture findings, senescent cholangiocytes may induce senescence in bystander cholangiocytes, thereby amplifying the senescent cell and SASP burden by way of paracrine signaling.<sup>41</sup> We have incorporated these findings and current hypotheses into a conceptual schematic model (Fig. 8). While the precise mechanisms of cholangiocyte senescence remain uncertain, we propose and are actively pursuing the concept that the increased accumulation of senescent cholangiocytes in PSC may result from: 1) a propensity for PSC cholangiocytes to initiate (and/or amplify) the senescent program; 2) inefficient clearance of senescent cholangiocytes; or 3) a combination of both. In addition, it should be noted that in this study we focused our *in vivo* experiments on small intrahepatic cholangiocytes. While we acknowledge that there is functional heterogeneity between small and large cholangiocytes,<sup>46</sup> we would predict that similar changes likely occur throughout the biliary tree.

Until now, very little has been reported regarding the presence and role of cellular senescence in the cholangiopathies. Sasaki et al.<sup>36</sup> were the first to explore the presence of cholangiocyte senescence markers in PBC and PSC livers and found a similarly increased proportion of senescent cholangiocytes in these two diseases as compared to other diseased and control livers. Our current work confirms the observation of senescent cholangiocytes in PSC and extends this by demonstrating the nonreplicative (i.e., stress-induced) type of cellular senescence in PSC, the cholangiocyte SASP phenotype in PSC, the ability of specific exogenous and endogenous molecules to induce senescence and SASP in human cholangiocytes, the capacity of senescent cholangiocytes to induce senescence in bystander

cells, and, finally, a mechanism (i.e., Ras activation) driving the senescent cholangiocyte phenotype (Fig. 8). In addition, our preliminary findings (data not shown) suggest that, consistent with the human data, cholangiocytes in a murine model of PSC (multidrug resistance 2 gene knockout, *mdr2*<sup>-/-</sup>)<sup>47</sup> also undergo senescence, thus providing a potential *in vivo* system for studying the pathological relevance of senescence in PSC.

In summary, we have demonstrated that cholangiocyte senescence and SASP are prominent in PSC, developed an *in vitro* model of NHC and bystander cell senescence, and initiated investigations relevant to the mechanisms of insult-induced cholangiocyte senescence. These insights may open the door to better understanding the etiopathogenesis of cholangiocyte senescence in the cholangiopathies, particularly PSC. Furthermore, they provide direction for targeted interventions in animal models (e.g., the *mdr2*<sup>-/-</sup> mouse) and potentially phase 1/2 clinical trials, which may include selective elimination of senescent cells (i.e., “senolytics”) or interference with the deleterious effects of the SASP.

## Supplementary Material

Refer to Web version on PubMed Central for supplementary material.

## Acknowledgments

Supported by National Institutes of Health grants AI089713 (to S.P.O.), DK57993 (to N.F.L), the Mayo Foundation, PSC Partners Seeking a Cure, and the Clinical and Optical Microscopy Cores of the Mayo Clinic Center for Cell Signaling in Gastroenterology (P30DK084567).

## Abbreviations

<b>CCA</b>	cholangiocarcinoma
<b>DDR</b>	DNA damage response
<b>HCV</b>	chronic hepatitis C
<b>IF</b>	immunofluorescence
<b>LPS</b>	lipopolysaccharide
<b>LT</b>	liver transplantation
<b>NHC</b>	normal human cholangiocyte
<b>PBC</b>	primary biliary cirrhosis
<b>PSC</b>	primary sclerosing cholangitis
<b>SA-β-gal</b>	senescence-associated β-gal
<b>SASP</b>	senescence-associated secretory phenotype
<b>TLR</b>	Toll-like receptor

## References

1. Tabibian JH, Lindor KD. Primary sclerosing cholangitis: a review and update on therapeutic developments. *Expert Rev Gastroenterol Hepatol.* 2013; 7:103–114. [PubMed: 23363260]

2. O'Hara SP, Tabibian JH, Splinter PL, Larusso NF. The dynamic biliary epithelia: molecules, pathways, and disease. *J Hepatol.* 2013; 58:575–582. [PubMed: 23085249]
3. Wiesner RH, Grambsch PM, Dickson ER, Ludwig J, MacCarty RL, Hunter EB, et al. Primary sclerosing cholangitis: natural history, prognostic factors and survival analysis. *Hepatology.* 1989; 10:430–436. [PubMed: 2777204]
4. Tabibian JH, Lindor KD. Challenges of cholangiocarcinoma detection in patients with primary sclerosing cholangitis. *J Anal Oncol.* 2012; 1:50–55.
5. Alabraba E, Nightingale P, Gunson B, Hubscher S, Olliff S, Mirza D, et al. A re-evaluation of the risk factors for the recurrence of primary sclerosing cholangitis in liver allografts. *Liver Transpl.* 2009; 15:330–340. [PubMed: 19243003]
6. Sasatomi K, Noguchi K, Sakisaka S, Sata M, Tanikawa K. Abnormal accumulation of endotoxin in biliary epithelial cells in primary biliary cirrhosis and primary sclerosing cholangitis. *J Hepatol.* 1998; 29:409–416. [PubMed: 9764987]
7. Mimura Y, Sakisaka S, Harada M, Sata M, Tanikawa K. Role of hepatocytes in direct clearance of lipopolysaccharide in rats. *Gastroenterology.* 1995; 109:1969–1976. [PubMed: 7498663]
8. O'Hara SP, Splinter PL, Trussoni CE, Gajdos GB, Lineswala PN, LaRusso NF. Cholangiocyte N-Ras protein mediates lipopolysaccharide-induced interleukin 6 secretion and proliferation. *J Biol Chem.* 2011; 286:30352–30360. [PubMed: 21757746]
9. Bansal AS, Thomson A, Steadman C, Le Gros G, Hogan PG, Kerlin P, et al. Serum levels of interleukins 8 and 10, interferon gamma, granulocyte-macrophage colony stimulating factor and soluble CD23 in patients with primary sclerosing cholangitis. *Autoimmunity.* 1997; 26:223–229. [PubMed: 9543183]
10. Karrar A, Broome U, Sodergren T, Jaksch M, Bergquist A, Bjornstedt M, et al. Biliary epithelial cell antibodies link adaptive and innate immune responses in primary sclerosing cholangitis. *Gastroenterology.* 2007; 132:1504–1514. [PubMed: 17408653]
11. Alvaro D, Mancino MG, Glaser S, Gaudio E, Marzioni M, Francis H, et al. Proliferating cholangiocytes: a neuroendocrine compartment in the diseased liver. *Gastroenterology.* 2007; 132:415–431. [PubMed: 17241889]
12. Mueller T, Beutler C, Pico AH, Shibolet O, Pratt DS, Pascher A, et al. Enhanced innate immune responsiveness and intolerance to intestinal endotoxins in human biliary epithelial cells contributes to chronic cholangitis. *Liver Int.* 2011; 31:1574–1588. [PubMed: 22093333]
13. Burton DG. Cellular senescence, ageing and disease. *Age (Dordr).* 2009; 31:1–9. [PubMed: 19234764]
14. Tchkonja T, Morbeck DE, Von Zglinicki T, Van Deursen J, Lustgarten J, Scoble H, et al. Fat tissue, aging, and cellular senescence. *Aging Cell.* 2010; 9:667–684. [PubMed: 20701600]
15. Campisi J, d'Adda di Fagagna F. Cellular senescence: when bad things happen to good cells. *Nat Rev Mol Cell Biol.* 2007; 8:729–740. [PubMed: 17667954]
16. Jeyapalan JC, Sedivy JM. Cellular senescence and organism aging. *Mech Ageing Dev.* 2008; 129:467–474. [PubMed: 18502472]
17. Coppe JP, Patil CK, Rodier F, Sun Y, Munoz DP, Goldstein J, et al. Senescence-associated secretory phenotypes reveal cell-nonautonomous functions of oncogenic RAS and the p53 tumor suppressor. *PLoS Biol.* 2008; 6:2853–2868. [PubMed: 19053174]
18. Trougakos IP, Saridaki A, Panayotou G, Gonos ES. Identification of differentially expressed proteins in senescent human embryonic fibroblasts. *Mech Ageing Dev.* 2006; 127:88–92. [PubMed: 16213575]
19. Kuilman T, Michaloglou C, Vredeveld LC, Douma S, van Doorn R, Desmet CJ, et al. Oncogene-induced senescence relayed by an interleukin-dependent inflammatory network. *Cell.* 2008; 133:1019–1031. [PubMed: 18555778]
20. Acosta JC, O'Loughlin A, Banito A, Guijarro MV, Augert A, Raguz S, et al. Chemokine signaling via the CXCR2 receptor reinforces senescence. *Cell.* 2008; 133:1006–1018. [PubMed: 18555777]
21. Serrano M, Lin AW, McCurrach ME, Beach D, Lowe SW. Oncogenic ras provokes premature cell senescence associated with accumulation of p53 and p16INK4a. *Cell.* 1997; 88:593–602. [PubMed: 9054499]

22. Ninlawan K, O'Hara SP, Splinter PL, Yongvanit P, Kaewkes S, Surapaitoon A, et al. Opisthorchis viverrini excretory/secretory products induce Toll-like receptor 4 upregulation and production of interleukin 6 and 8 in cholangiocyte. *Parasitol Int.* 2010; 59:616–621. [PubMed: 20887801]
23. Lopez de Padilla CM, Vallejo AN, McNallan KT, Vehe R, Smith SA, Dietz AB, et al. Plasmacytoid dendritic cells in inflamed muscle of patients with juvenile dermatomyositis. *Arthritis Rheum.* 2007; 56:1658–1668. [PubMed: 17469160]
24. Erickson HS, Albert PS, Gillespie JW, Rodriguez-Canales J, Marston Linehan W, Pinto PA, et al. Quantitative RT-PCR gene expression analysis of laser microdissected tissue samples. *Nat Protoc.* 2009; 4:902–922. [PubMed: 19478806]
25. O'Hara SP, Bogert PS, Trussoni CE, Chen X, LaRusso NF. TLR4 promotes *Cryptosporidium parvum* clearance in a mouse model of biliary cryptosporidiosis. *J Parasitol.* 2011; 97:813–821. [PubMed: 21506806]
26. Agle CC, Velloso CP, Lazarus NR, Harridge SD. An image analysis method for the precise selection and quantitation of fluorescently labeled cellular constituents: application to the measurement of human muscle cells in culture. *J Histochem Cytochem.* 2012; 60:428–438. [PubMed: 22511600]
27. Wang C, Jurk D, Maddick M, Nelson G, Martin-Ruiz C, von Zglinicki T. DNA damage response and cellular senescence in tissues of aging mice. *Aging Cell.* 2009; 8:311–323. [PubMed: 19627270]
28. Meeker AK, Gage WR, Hicks JL, Simon I, Coffman JR, Platz EA, et al. Telomere length assessment in human archival tissues: combined telomere fluorescence in situ hybridization and immunostaining. *Am J Pathol.* 2002; 160:1259–1268. [PubMed: 11943711]
29. van Heek NT, Meeker AK, Kern SE, Yeo CJ, Lillemoe KD, Cameron JL, et al. Telomere shortening is nearly universal in pancreatic intraepithelial neoplasia. *Am J Pathol.* 2002; 161:1541–1547. [PubMed: 12414502]
30. Sasaki M, Ikeda H, Yamaguchi J, Nakada S, Nakanuma Y. Telomere shortening in the damaged small bile ducts in primary biliary cirrhosis reflects ongoing cellular senescence. *Hepatology.* 2008; 48:186–195. [PubMed: 18536059]
31. de Planell-Saguer M, Rodicio MC, Mourelatos Z. Rapid in situ codetection of noncoding RNAs and proteins in cells and formalin-fixed paraffin-embedded tissue sections without protease treatment. *Nat Protoc.* 2010; 5:1061–1073. [PubMed: 20539282]
32. Banales JM, Saez E, Uriz M, Sarvide S, Urribarri AD, Splinter P, et al. Up-regulation of microRNA 506 leads to decreased Cl<sup>-</sup>/HCO<sub>3</sub><sup>-</sup> anion exchanger 2 expression in biliary epithelium of patients with primary biliary cirrhosis. *Hepatology.* 2012; 56:687–697. [PubMed: 22383162]
33. Dimri GP, Lee X, Basile G, Acosta M, Scott G, Roskelley C, et al. A biomarker that identifies senescent human cells in culture and in aging skin in vivo. *Proc Natl Acad Sci U S A.* 1995; 92:9363–9367. [PubMed: 7568133]
34. Lawless C, Wang C, Jurk D, Merz A, Zglinicki T, Passos JF. Quantitative assessment of markers for cell senescence. *Exp Gerontol.* 2010; 45:772–778. [PubMed: 20117203]
35. Sasaki M, Miyakoshi M, Sato Y, Nakanuma Y. Modulation of the micro-environment by senescent biliary epithelial cells may be involved in the pathogenesis of primary biliary cirrhosis. *J Hepatol.* 2010; 53:318–325. [PubMed: 20570384]
36. Sasaki M, Ikeda H, Haga H, Manabe T, Nakanuma Y. Frequent cellular senescence in small bile ducts in primary biliary cirrhosis: a possible role in bile duct loss. *J Pathol.* 2005; 205:451–459. [PubMed: 15685690]
37. Lichtman SN, Keku J, Clark RL, Schwab JH, Sartor RB. Biliary tract disease in rats with experimental small bowel bacterial overgrowth. *Hepatology.* 1991; 13:766–772. [PubMed: 2010172]
38. Lichtman SN, Keku J, Schwab JH, Sartor RB. Hepatic injury associated with small bowel bacterial overgrowth in rats is prevented by metronidazole and tetracycline. *Gastroenterology.* 1991; 100:513–519. [PubMed: 1985047]
39. Park J, Gores GJ, Patel T. Lipopolysaccharide induces cholangiocyte proliferation via an interleukin-6-mediated activation of p44/p42 mitogen-activated protein kinase. *Hepatology.* 1999; 29:1037–1043. [PubMed: 10094943]

40. Gosselin K, Deruy E, Martien S, Vercamer C, Bouali F, Dujardin T, et al. Senescent keratinocytes die by autophagic programmed cell death. *Am J Pathol.* 2009; 174:423–435. [PubMed: 19147823]
41. Nelson G, Wordsworth J, Wang C, Jurk D, Lawless C, Martin-Ruiz C, et al. A senescent cell bystander effect: senescence-induced senescence. *Aging Cell.* 2012; 11:345–349. [PubMed: 22321662]
42. Sokolov MV, Smilenov LB, Hall EJ, Panyutin IG, Bonner WM, Sedelnikova OA. Ionizing radiation induces DNA double-strand breaks in bystander primary human fibroblasts. *Oncogene.* 2005; 24:7257–7265. [PubMed: 16170376]
43. Hayflick L. The limited in vitro lifetime of human diploid cell strains. *Exp Cell Res.* 1965; 37:614–636. [PubMed: 14315085]
44. Harper JW, Elledge SJ. The DNA damage response: ten years after. *Mol Cell.* 2007; 28:739–745. [PubMed: 18082599]
45. Rodier F, Campisi J. Four faces of cellular senescence. *J Cell Biol.* 2011; 192:547–556. [PubMed: 21321098]
46. Kanno N, LeSage G, Glaser S, Alvaro D, Alpini G. Functional heterogeneity of the intrahepatic biliary epithelium. *Hepatology.* 2000; 31:555–561. [PubMed: 10706542]
47. Tabibian JH, Macura SI, O'Hara SP, Fidler JL, Glockner JF, Takahashi N, et al. Micro-computed tomography and nuclear magnetic resonance imaging for noninvasive, live-mouse cholangiography. *Lab Invest.* 2013; 93:733–743. [PubMed: 23588707]

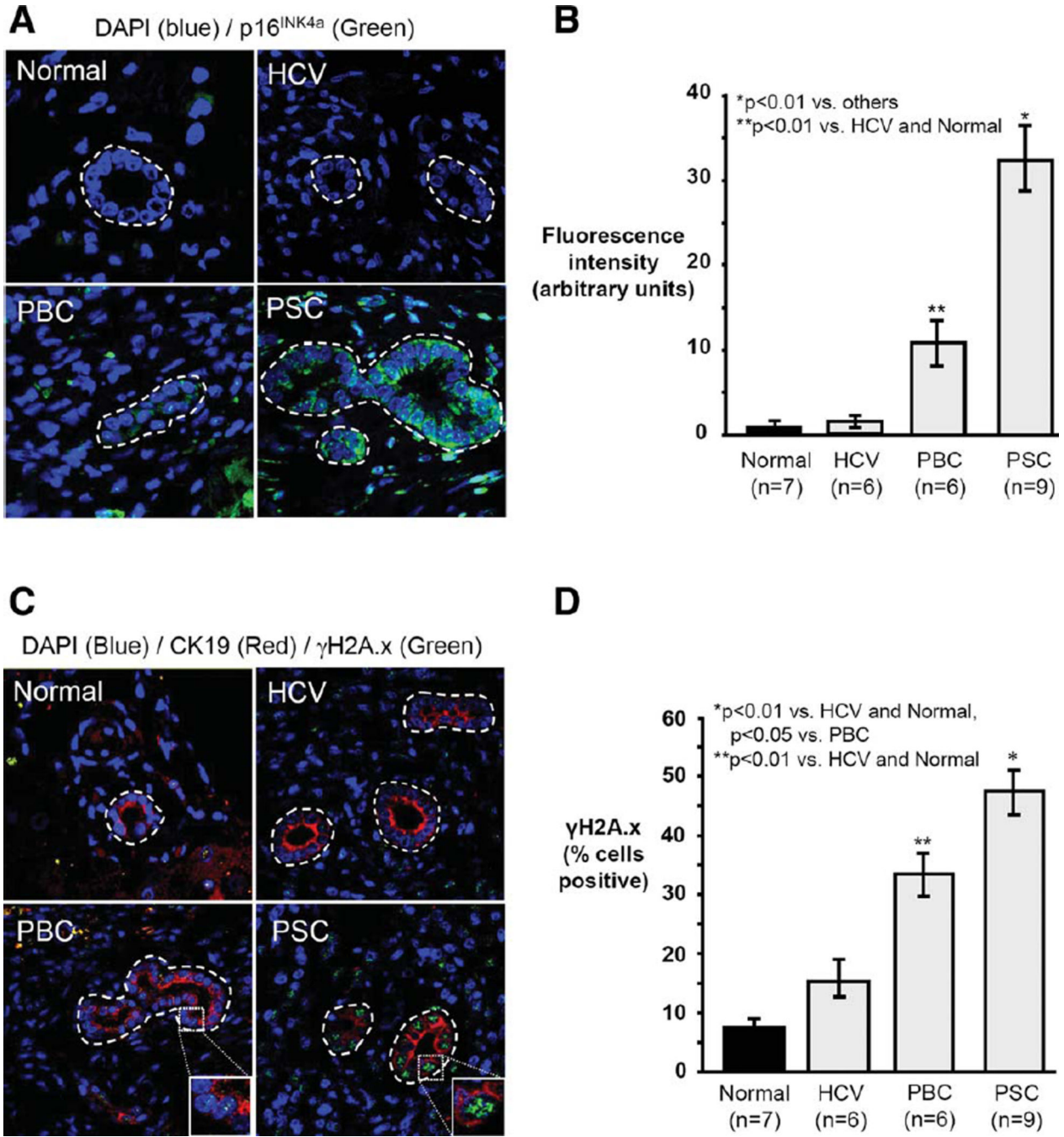


**Fig. 1.** Cholangiocytes in PSC liver exhibit increased markers of cellular senescence. (A) Representative images of p16<sup>INK4A</sup> mRNA FISH (p16<sup>INK4A</sup> probe = green; DAPI = blue). (B) Semiquantitative analysis of fluorescence intensity demonstrates significantly increased cholangiocyte p16<sup>INK4A</sup> in PSC compared to other conditions. (C) Representative images of  $\gamma$ H2A.x immunofluorescence ( $\gamma$ H2A.x = green; DAPI = blue). (D) Quantitation of  $\gamma$ H2A.x foci demonstrates a higher proportion of  $\gamma$ H2A.x-positive cholangiocytes in PSC compared to other conditions.

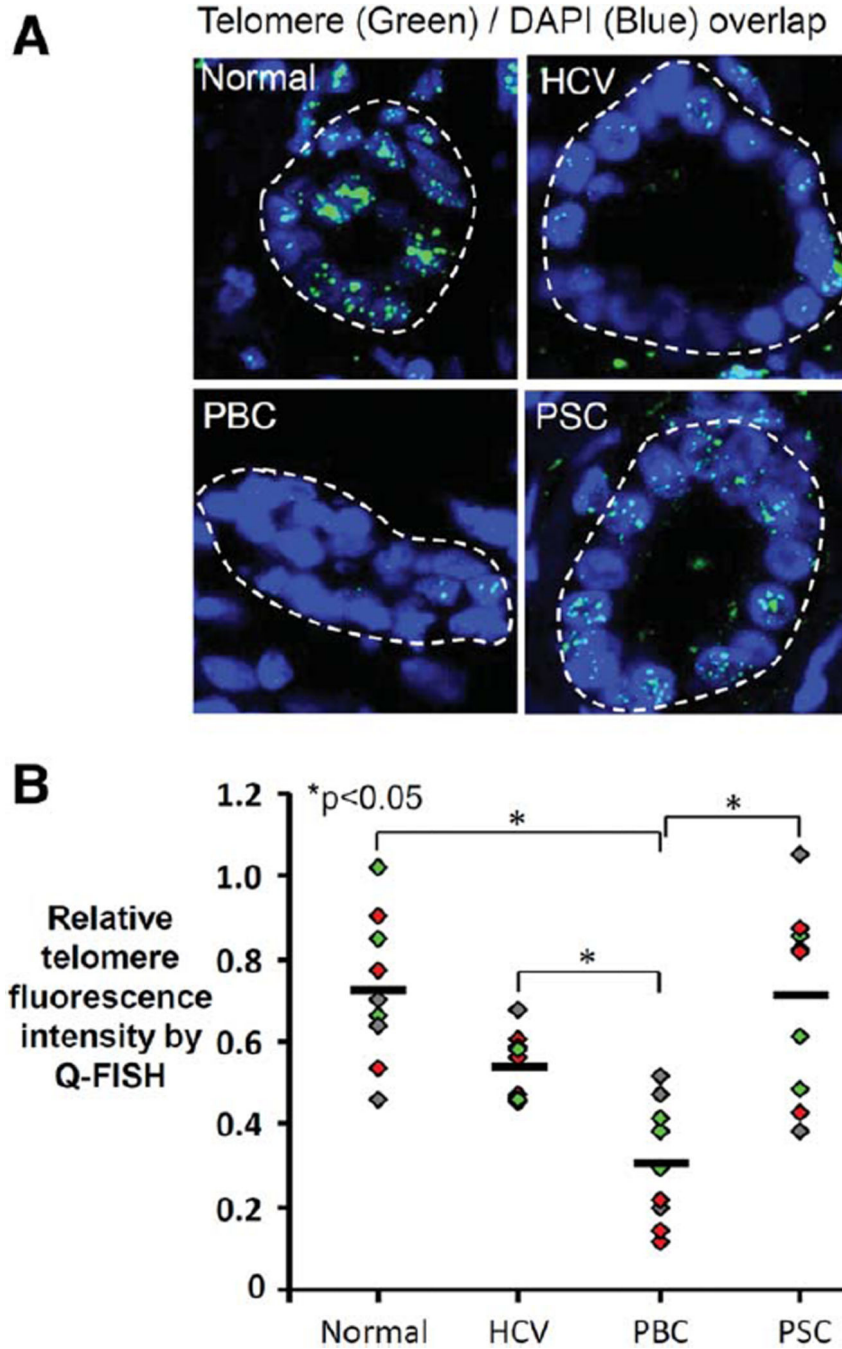


**Fig. 2.** Telomere length is preserved in PSC cholangiocytes. (A) Representative confocal fluorescence images of Tel-C-FITC FISH performed on liver sections to assess cholangiocyte telomere length. (B) Cholangiocyte telomere fluorescence intensity is similar in PSC and normal liver but significantly decreased in PBC. Diamonds represent the average relative telomere fluorescence intensity of bile ducts in a randomly selected liver section (three sections assessed in each of three patients, each patient shown in a different color); horizontal line represents the average of the three patients in each condition. For analysis,



three average values were used for each patient based on the three randomly selected liver sections that were assessed. If per-patient average values are used instead of per-section average values, the difference between HCV and PBC loses statistical significance, while the difference between PSC and PBC and the difference between normal and PBC retain statistical significance (both  $P < 0.05$ ).

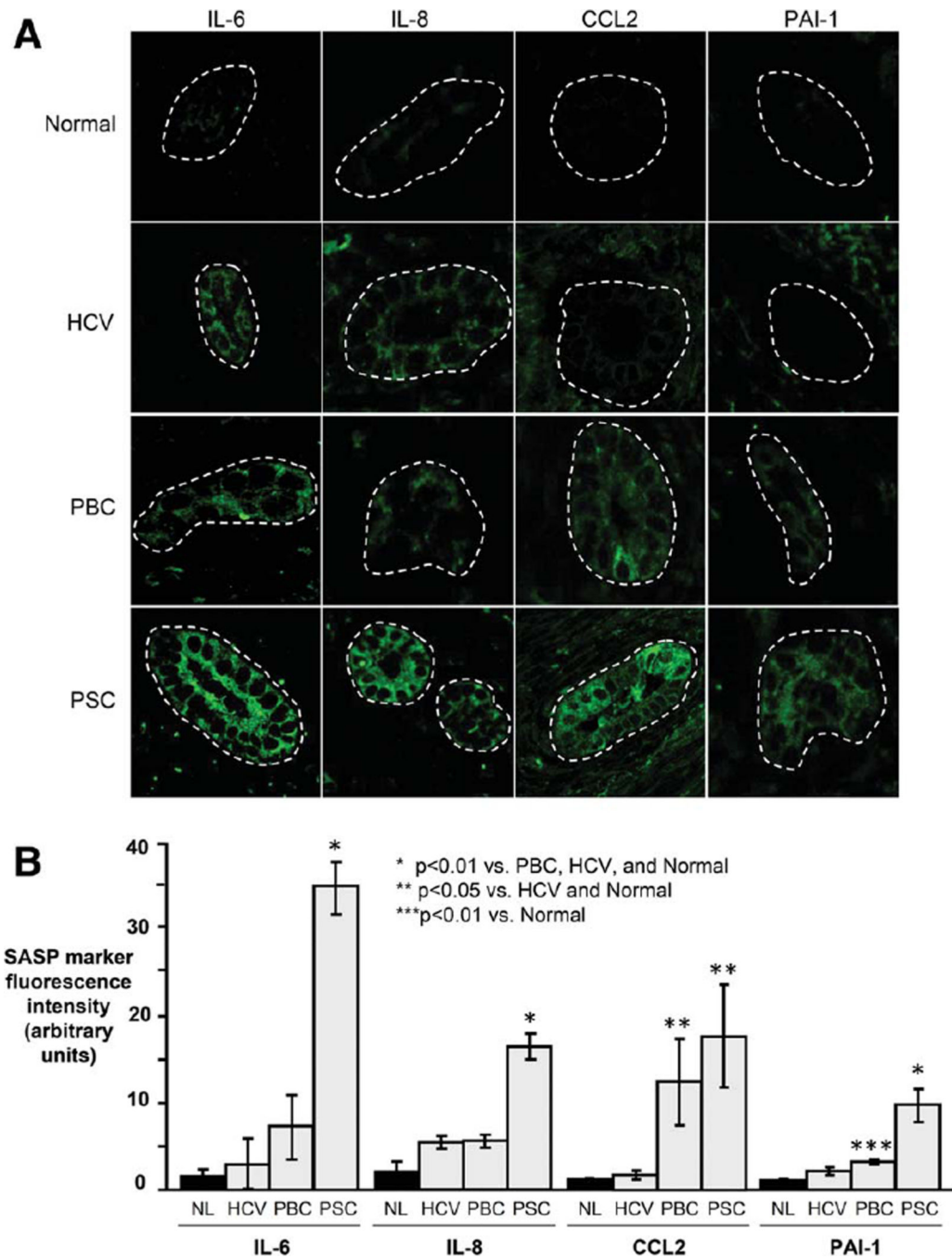


**Fig. 3.** Cholangiocytes in PSC liver exhibit increased expression of SASP components. (A) Representative images of IL-6, IL-8, CCL2, and PAI-1 immunofluorescence in liver sections. (B) Semi-quantitative analysis of fluorescence intensity (presented as arbitrary units) demonstrates significantly increased cholangiocyte expression of SASP components in PSC.

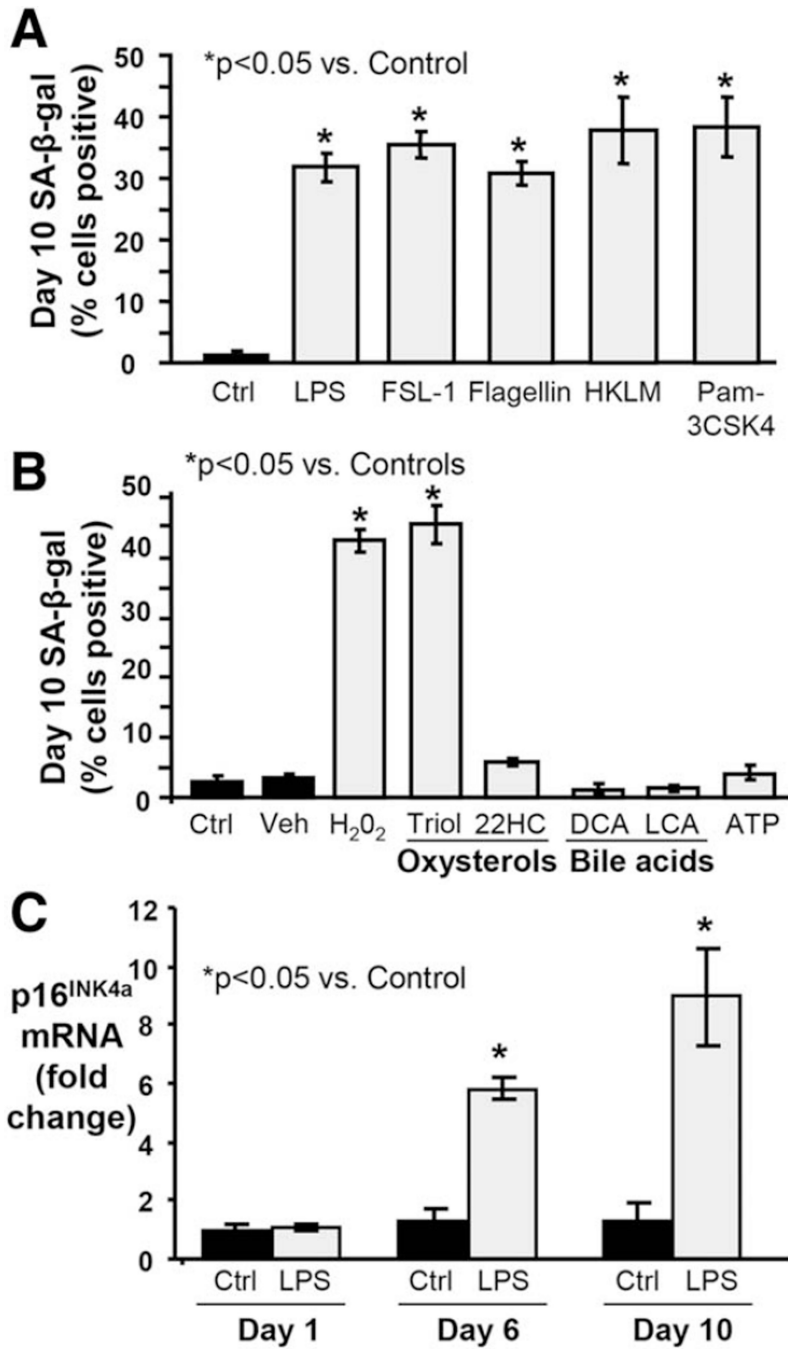


**Fig. 4.** *In vitro* model of stress-induced NHC senescence by persistent treatment with exogenous and endogenous insults. NHCs were exposed to exogenous (i.e., microbially derived) and endogenous stressors over the course of 10 days. (A) The proportion of SA-β-gal-positive NHCs increases following 10-day treatment with exogenous stressors, indicating induction of senescence. FSL-1, synthetic diacylated lipoprotein; HKLM, heat-killed *L. monocytogenes*; Pam3CSK4, synthetic triacylated lipoprotein. (B) The proportion of SA-β-gal-positive NHCs increases following 10-day treatment with (some) endogenous stressors,

indicating induction of senescence. Veh, vehicle (ethanol) for Triol (cholestane-3 $\beta$ , 5 $\alpha$ , 6 $\alpha$ -triol); 22HC, 22-hydroxycholesterol; DCA, deoxycholic acid; LCA, lithocholic acid; ATP, adenosine triphosphate. (C) Persistent LPS treatment induces significantly increased p16<sup>INK4a</sup> mRNA expression at day 6 day and a further increase at day 10 compared to control cells.

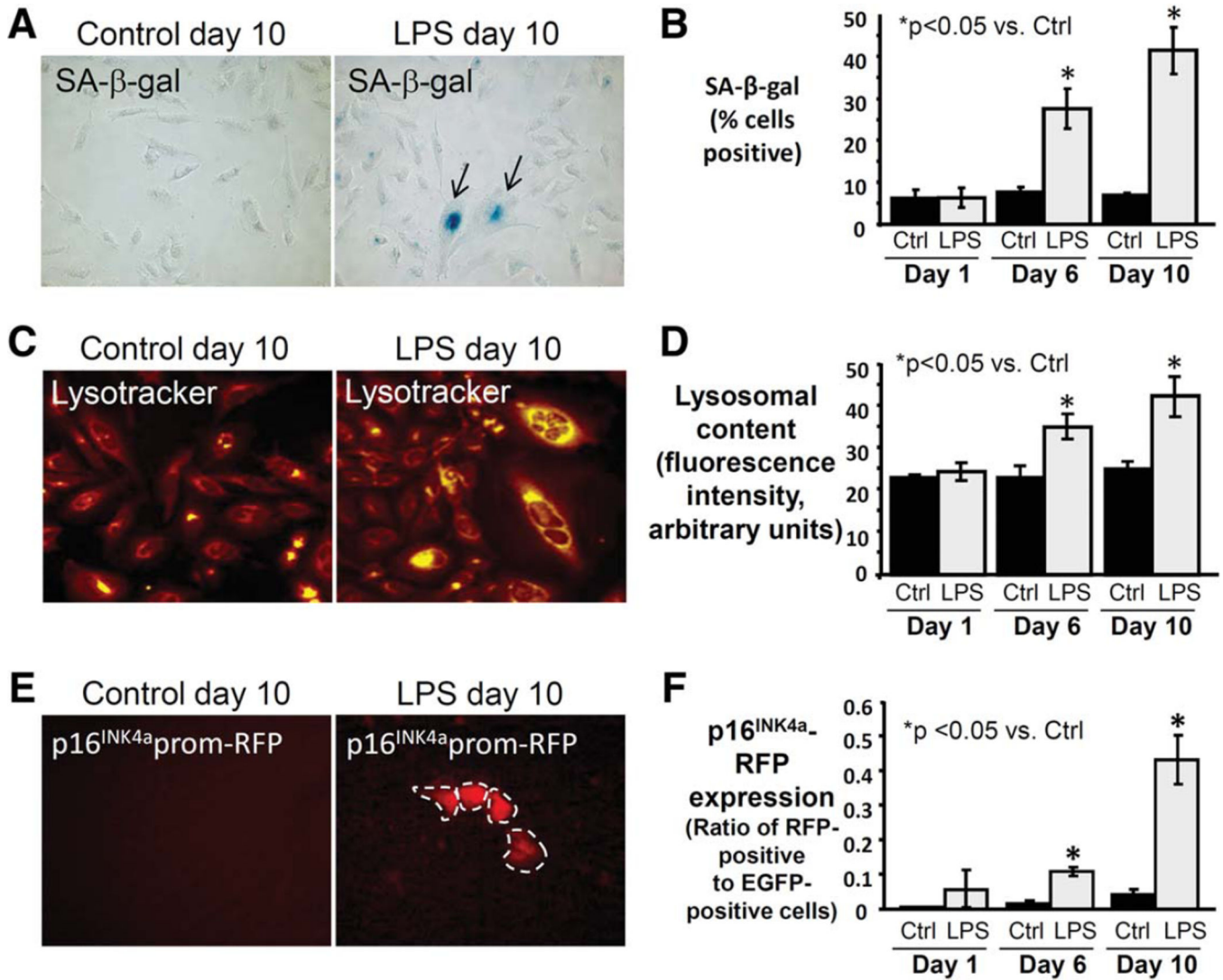


**Fig. 5.** Persistent treatment with LPS induces expression of multiple senescence markers in NHCs. (A) Representative brightfield microscopy images at day 10 demonstrating increased LPS-induced SA-β-gal and cytologic features of senescence (larger size, squamoid appearance). (B) SA-β-gal quantitation reveals significantly increased proportion of SA-β-gal-positive NHCs following 6 and 10 days of LPS treatment. (C) Representative images at day 10 demonstrating increased LPS-induced lysosomal content. (D) Quantitation of lysosomal content reveals a significant increase in lysosomal content at day 6 and a further increase at day 10 compared to control. (E) Representative images at day 10 demonstrating LPS-induced expression of p16<sup>INK4a</sup> promoter-driven reporter (RFP). (F) Quantitation of p16<sup>INK4a</sup> (presented as the ratio of RFP to EGFP-positive cells) confirms a significant increase at day 6 and a further increase at day 10 compared to control.

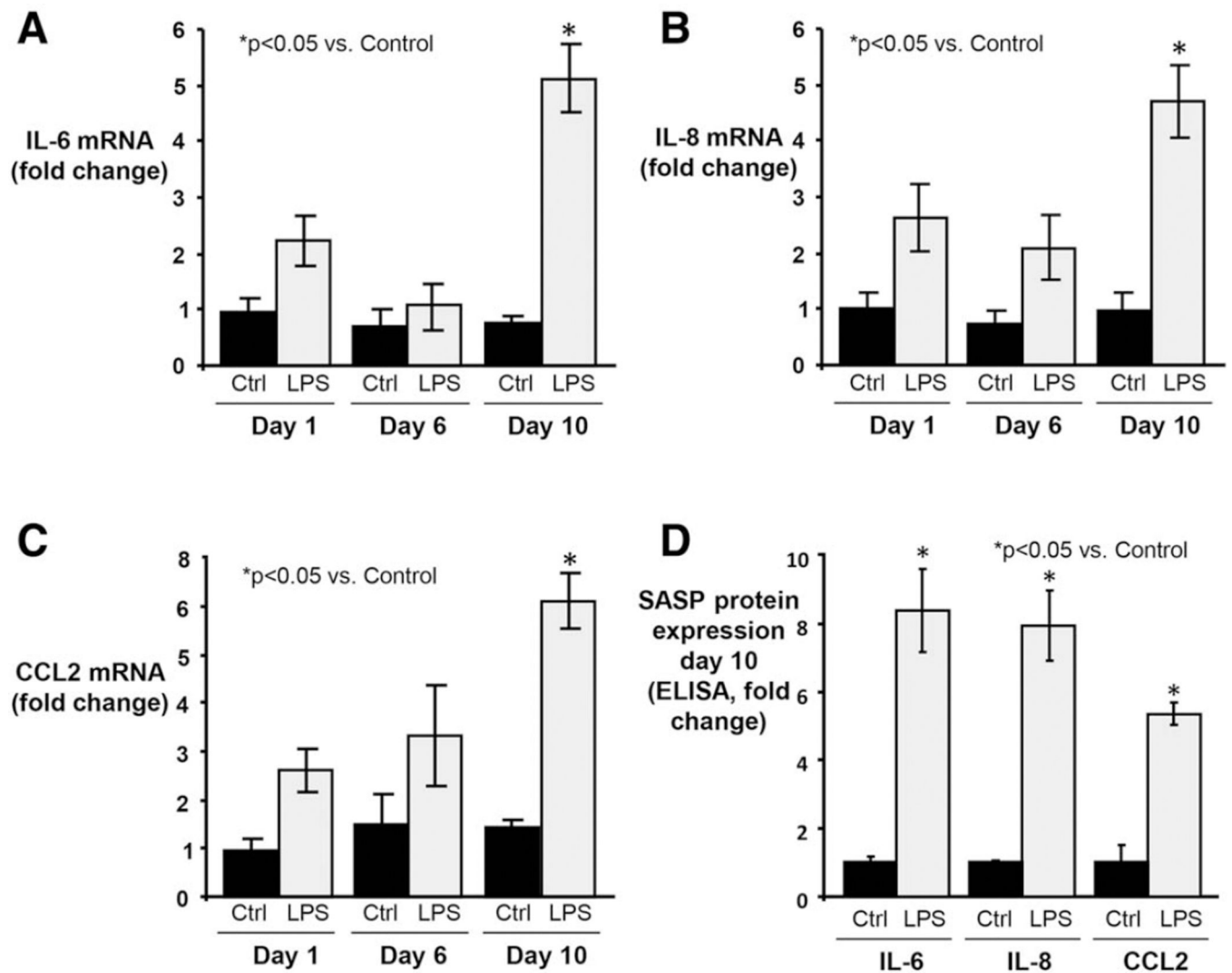


**Fig. 6.** Persistent LPS treatment of NHCs induces expression of SASP components. (A) IL-6 mRNA expression was assessed by qPCR at 1, 6, and 10 days of LPS treatment. By day 10, expression is significantly elevated (~5-fold > control; ~2-fold > 1 day LPS-treatment). (B) IL-8 mRNA expression is significantly increased by day 10 (~5-fold > control; ~1.5-fold > 1 day LPS-treatment). The delayed response observed in IL-8 (as well as IL-6) expression following an initial acute response is consistent with the time-dependent induction of senescence as demonstrated in other cell types and culture models.<sup>33</sup> (C) CCL2 mRNA expression is significantly increased by day 10 (~4.7-fold > control; ~1.9-fold > 1 day LPS-treatment). (D) ELISA of conditioned media from 10-day LPS-treated NHCs demonstrating significantly increased IL-6, IL-8, and CCL2 protein expression compared to control.

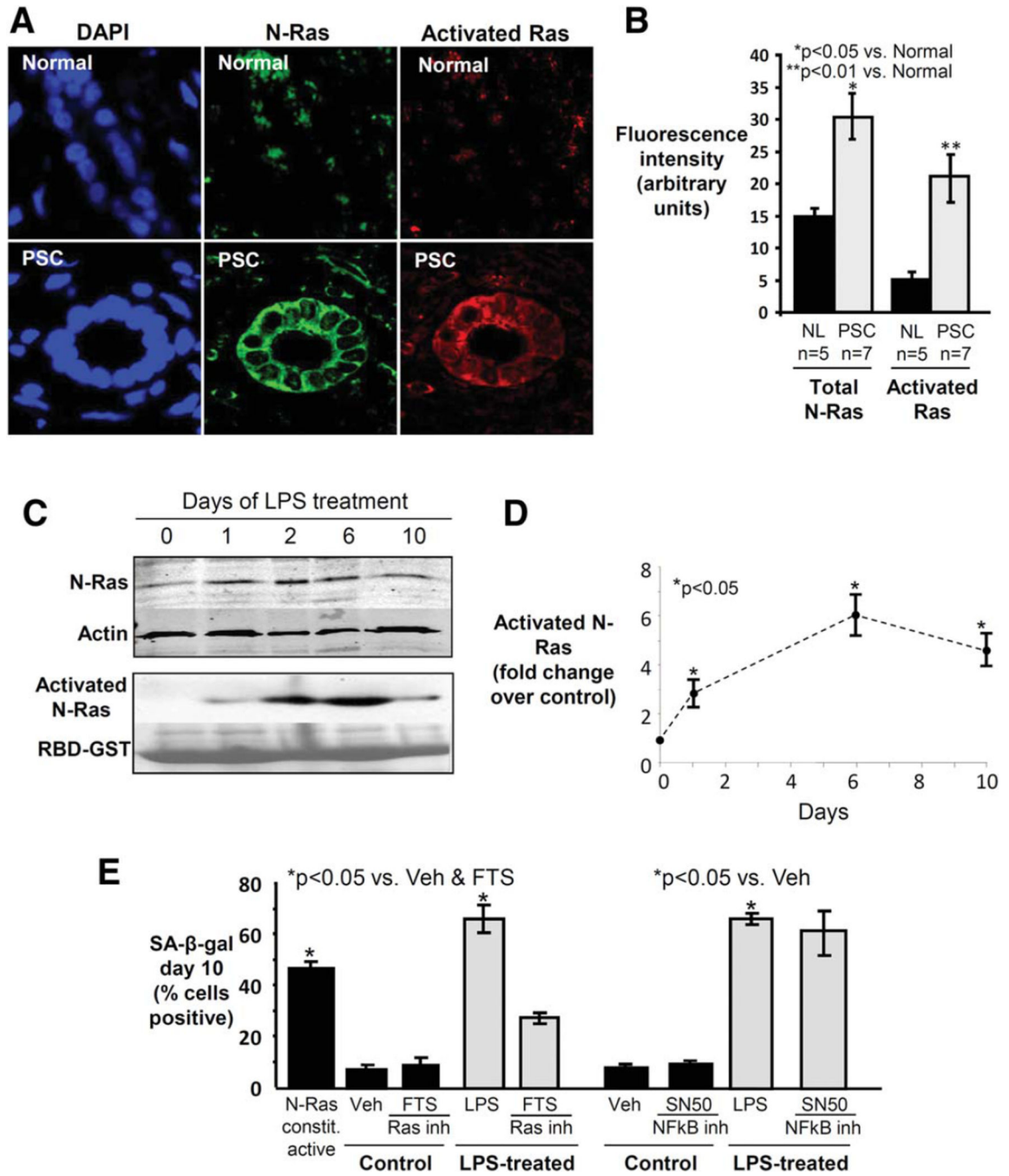


**Fig. 7.** Ras is activated in cholangiocytes in PSC liver, and Ras activation is involved in LPS-induced NHC senescence. (A) Representative con-focal immunofluorescence images for N-Ras (green) and activated Ras (red) (DAPI = blue). Cholangiocyte N-Ras colocalizes with activated Ras in PSC liver, suggesting that N-Ras is not only expressed, but also activated in PSC cholangiocytes. (B) Semiquantitative analysis of fluorescence demonstrates significantly increased N-Ras and activated Ras in PSC cholangiocytes compared to normal. (C) LPS treatment of NHCs induces persistent N-Ras activation. Western blot demonstrates

cholangiocyte N-Ras expression, and an RBD-GST pulldown demonstrates LPS-induced Ras activation over the course of 10 days (Ponceau Red used to stain total RBD-GST, loading control). (D) Densitometry on the activated N-Ras blot at each time point. (E) Ras, but not NF- $\kappa$ B inhibition, decreases LPS-induced cholangiocyte senescence. NHCs were cultured in the presence or absence of LPS and a Ras (FTS) or NF- $\kappa$ B (SN50) inhibitor. Cholangiocyte senescence, determined by proportion of SA- $\beta$ -gal-positive cholangiocytes, is abrogated by Ras inhibition.



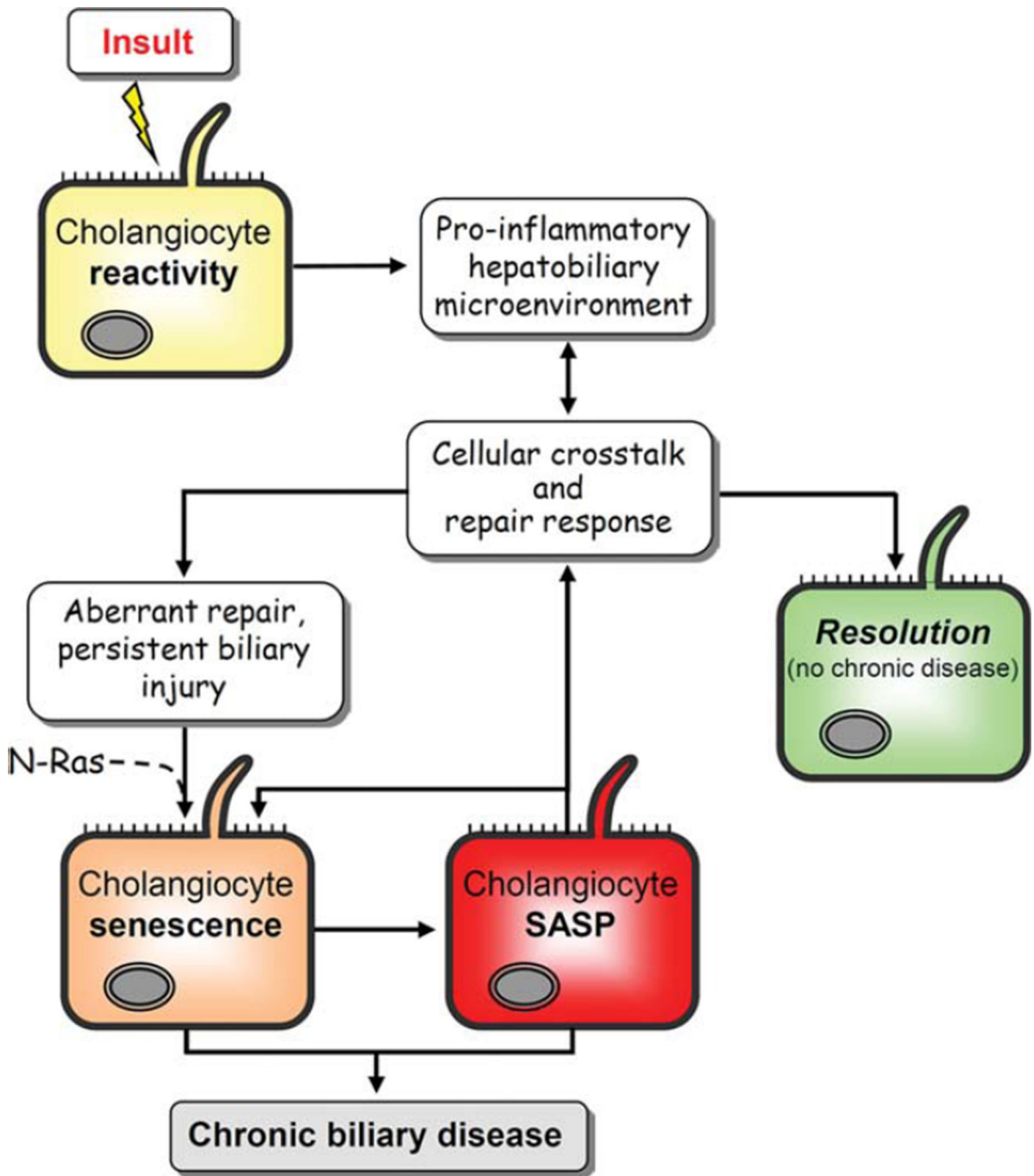


**Fig. 8.** Conceptual framework of PSC pathogenesis. In this working model, the cholangiocyte is exposed to endogenous and/or exogenous insults to which it responds through up-regulation of proinflammatory mediators as characteristic of a “reactive cholangiocyte.” This process initiates intricate crosstalk between a variety of resident and recruited cells, including hepatocytes, progenitor cells, fibroblasts, and leukocytes, in an attempt to resolve injury and repair the biliary epithelium. In immunogenetically susceptible individuals, the proinflammatory response of and injury to cholangiocytes do not resolve. Instead, as a result

of aberrant genomic and cellular repair, we speculate, based on our data and current hypotheses, that there is induction of N-Ras mediated, insult-induced cholangiocyte senescence. Senescent cholangiocytes can then progress to SASP, a potentially pathologic state characterized by hypersecretion of proinflammatory cytokines (e.g., IL-6) and chemokines (e.g., IL-8) and profibrotic mediators (e.g., PAI-1), as shown in the present study. By way of these secreted mediators, SASP cells have been shown to alter their microenvironment, reinforce the senescent phenotype, and exacerbate injurious fibroinflammatory responses which, in the liver, results in progressive injury and ultimately chronic biliary disease (i.e., PSC).